

Entanglement scaling for $\lambda\phi^4$

Bram Vanhecke[✉], Frank Verstraete, and Karel Van Acoleyen*Department of Physics and Astronomy, University of Ghent, Krijgslaan 281, 9000 Gent, Belgium* (Received 25 June 2021; accepted 28 September 2022; published 20 October 2022)

We study the $\lambda\phi^4$ model in $0 + 2$ dimensions at criticality, focusing on the scaling properties originating from the UV and IR physics. We demonstrate that the entanglement entropy, the correlation length ξ and order parameters ϕ and ϕ^3 exhibit distinctive double scaling properties that prove a powerful tool in the data analysis. The calculations are performed with boundary matrix product state methods on tensor network representations of the partition function to which the entanglement scaling hypothesis is applied, though the technique is equally applicable outside the realm of tensor networks. We find the value $\alpha_c = 11.09698(31)$ for the critical point, improving on previous results.

DOI: [10.1103/PhysRevD.106.L071501](https://doi.org/10.1103/PhysRevD.106.L071501)

I. INTRODUCTION

Scaling is one of the most profound concepts in modern day physics, as it plays a crucial role in the understanding and simulation of many-body systems that exhibit critical infrared (IR) behavior [1–3]. Furthermore, for quantum field theories (QFTs) defined through lattice regularization, the continuum limit emerges precisely in the scaling behavior towards the ultraviolet (UV) critical point [4–7]. In this context, QFTs with a second-order phase transition—of which $D = 2$ $\lambda\phi^4$ is the archetypal example—hold a particular place. They are subject to both types of scaling, with the UV scaling defining the continuum limit, and the IR scaling near the QFT phase transition, each characterized by their own distinct CFT.

The typical procedure to study such a model with double critical behavior is to choose some values of the UV cutoff, for each of them determine the effective critical point, and extrapolate. Calculating all these critical points goes exactly as one would for any lattice model, typically using the IR scaling properties, through distinct power-laws or scaling hypotheses [8–11]. It should thus be clear that each of those effective critical points are expensive to calculate, requiring many different values of the coupling and the IR cutoff (typically system size L , or in tensor network studies a bond dimension χ). Further more, such an approach leaves questions about the interplay between the UV and IR CFTs untouched and all its possible benefits unused.

In this paper we will investigate how one could go about leveraging both the UV and IR scaling properties, to simultaneously use all data points in one fit for the continuum critical point. The technique builds and improves upon a previous work [12] and entails constructing quantities that are scale invariant with respect to both the IR and UV scaling, using them to effectuate a double collapse of all the data. This proves an effective way to fit the data and also captures and visualizes the ways that the UV and IR CFTs manifest themselves.

Numerical calculations are done within the tensor network (TN) framework; the regularized model is expressed as a square lattice TN that is contracted by determining the approximate matrix product state [13] (MPS) fixed point of the matrix product operator [14] (MPO) transfer matrix, with the variational uniform matrix product state [15] algorithm. The finite bond dimension of the MPS introduces finite entanglement effects similar to finite size effects [16–19]. In the entanglement scaling hypothesis [12] for MPS, a quantity, δ , is identified which acts as an inverse system size L^{-1} under scaling, and can be used as a substitute for χ to label the MPS results. The finite bond dimension effects will thus be handled using the scaling properties, in exactly the same way as one would for calculations performed at finite size [3]. Our analysis can thus be straightforwardly applied to Hamiltonian methods [20] or approaches based on the corner transfer matrix method (CTM) [21–23], for which the entanglement scaling hypothesis also holds, and furthermore our method can be trivially adapted to methods with finite lattice size effects like Monte Carlo or exact diagonalization.

We will first review the model, then construct the aforementioned scale invariant quantities, and finally, we discuss the results obtained by optimizing the collapses.

Published by the American Physical Society under the terms of the Creative Commons Attribution 4.0 International license. Further distribution of this work must maintain attribution to the author(s) and the published article's title, journal citation, and DOI. Funded by SCOAP³.

II. THE MODEL

We start from the Euclidean action

$$\mathcal{L}(\phi) = \frac{1}{2} \partial_\mu \phi \partial^\mu \phi + \frac{1}{2} \mu_0^2 \phi^2 + \frac{1}{4} \lambda_0 \phi^4, \quad (1)$$

where ϕ is a real function of $2-D$ space. This is a superrenormalizable QFT at the perturbative level [24] and it has been proven [25] that this model gives rise to a nontrivial theory at the full nonperturbative level. The model has a \mathbb{Z}_2 symmetry-breaking phase transition in the Ising universality class, at a coupling that is beyond the reach of standard perturbation theory.

We study this model using lattice regularization, discretizing both space and time.

$$Z = \int \prod_i d\phi_i e^{-\sum_{(i,j)} \frac{1}{2} (\phi_i - \phi_j)^2 - \sum_i \frac{1}{2} \mu^2 \phi_i^2 + \frac{1}{4} \lambda \phi_i^4}, \quad (2)$$

The above partition function can be written as a tensor network of finite bond dimension by discretizing ϕ_i , the details of which are in the Supplemental Material [26]. Different than previous approaches [27,28], our approach is distinguished by arbitrary precision, optimal-bond dimension, and minimal computational cost.

III. CONTINUUM LIMIT

To extract the continuum theory from this lattice model one should vary the parameters μ and λ such that every conceivable linear length scale (i.e., masses, scattering lengths,...) becomes proportional to all others as they diverge. From perturbation theory we get the precise prescription for taking this QFT continuum limit [28],

$$\begin{aligned} \mu^2 &= \lambda \alpha - 3\lambda A(\lambda \alpha) \\ A(x) &= \int_0^\pi \int_0^\pi \frac{dy dz}{x + 4 \sin(y)^2 + 4 \sin(z)^2} \\ a^2 &= \lambda, \end{aligned} \quad (3)$$

where a is the effective lattice spacing in real space units. The function $A(x)$ originates from the (one-loop) tadpole diagram of the mass renormalization for our particular lattice regularization. For each α the above expression parametrizes a continuum limit, prescribing how μ and λ should be varied to take the effective lattice spacing a to zero while preserving all correlations in real space units. See the illustration in Fig. 1. It is important to realize that the parameter α is universal, in the sense that it may be compared across different regularization schemes, it is usually denoted μ_R/λ .

The presence of a second order phase transition of the QFT implies that the continuum correlation length $= \lim_{a \rightarrow 0} a \xi(a, \alpha)$ diverges as α is tuned to the critical value α_c . For the lattice model of Eq. (2) this means there must be

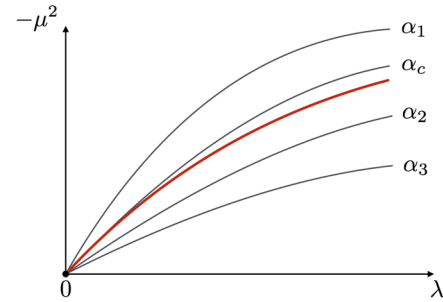


FIG. 1. Sketch of the phase diagram of the lattice model (2) in the $(-\mu^2, \lambda)$ plane, with the critical line in red, and also some lines describing different continuum limits [Eq. (3)]. The prime goal of our simulations is to find the critical α_c , for which the continuum limit converges to the critical line for $a \rightarrow 0$.

a critical line in the (μ^2, λ) -plane that is parametrized by α_c , up to leading order in a . However, at $a \gg 0$, there will be finite cutoff effects that make this critical line deviate from a curve of constant α , effectively causing the critical value of α to shift with λ . This is illustrated in Fig. 1.

This issue cannot be overcome by simply working with small enough λ as the gains in decreased finite cutoff effects are vastly outweighed by the added computational cost. We will thus work with small but reasonable λ data and fit the subleading corrections that should be added to the definition of α , in Eq. (3), that are required to make the critical point constant with λ .

First, though, we will ignore these complications and build a scaling theory around $a \approx 0$ and $\alpha \approx \alpha_c$, and later add the necessary corrections. We will use the scaling properties of the UV, which follow from the existence of a continuum limit, and the scaling properties of the IR, caused by the second order phase transition, to collapse 3D data $O(\mu^2, \lambda, \chi)$ to a 1D curve $\tilde{O}(\alpha)$.

IV. DOUBLE SCALING: UV AND IR

To do a UV scale transformation one should imagine doing a renormalization group transformation as generally appearing in QFT; rescaling the cutoff, here the lattice spacing a , while keeping the continuum quantities fixed. The exponents of all the variables and observables are then determined by their response to such a transformation (up to leading order in a).

It thus follows from Eq. (3) that λ has UV scaling exponent 2, and α has exponent 0. The lattice-correlation length ξ has UV exponent -1 , since $a\xi$ —the continuum correlation length—must remain constant when varying a . And, similarly the inverse linear system size L^{-1} (in lattice units), or its MPS counterpart δ , has exponent 1.

Since there is no wave function renormalization needed for ϕ_2^4 in the continuum limit, the UV exponent of the field ϕ is simply 0, corresponding to its canonical dimension. To extend the number of observables, we have also considered

the composite operator ϕ^3 . As such this operator is not properly defined for the QFT, as it has a UV divergence, arising from the tadpole contribution to the disconnected part, which evaluates to $3\langle\phi^2\rangle\times\phi\sim-\frac{3}{4\pi}\log(\lambda)\phi$ (see Supplemental Material [26]). We therefore subtract this divergence to define a regularized $\tilde{\phi}^3 = \phi^3 + \frac{3}{4\pi}\log(\lambda)\phi$. This finite operator $\tilde{\phi}^3$ then scales according to its canonical dimension, which is again 0.

Finally, we have also considered the entanglement entropy S as a QFT observable [29]. From the diverging lattice correlation length at fixed α in the $a \rightarrow 0$ limit, and the Cardy-Calabrese [31] entanglement law we can anticipate $S \sim -\frac{c_{uv}}{6}\log(a)$, with c_{uv} the central charge of the free boson CFT $c_{uv} = 1$. By formally considering the quantity e^S , we can translate this logarithmic scaling to a UV-exponent $-\frac{c_{uv}}{6}$.

Next, we consider the IR scaling, which can be understood as an renormalization group-flow of the continuum theory. The IR exponent of λ is 0 as the continuum theory is independent of the lattice spacing $a = \sqrt{\lambda}$. The exponent $1/\nu$ of $\alpha - \alpha_c$ acts as temperature does in the Ising model. Regular lengths have their usual exponent, so the correlation length has IR exponent -1 , and L^{-1} and δ have exponent 1. As was found for the UV scaling of e^S , we similarly find that the IR exponent of e^S should be $-\frac{c_{ir}}{6}$, where $c_{ir} = 1/2$ is the central charge of the Ising CFT. Finally, the observables ϕ and ϕ^3 , and thus also $\tilde{\phi}^3$, act as \mathbb{Z}_2 order parameters with respect to the Ising critical point. They therefore have IR exponent β , which in this case is $1/8$. See Table I, for all UV and IR exponents.

We are now ready to construct scale invariant quantities from our four observables $O = \xi, \phi, \tilde{\phi}^3, e^S$. This is achieved by compensating for the UV exponent with appropriate factors of $\sqrt{\lambda}$ (the lattice spacing) and similarly for the IR exponent with factors of $\Delta = \delta/\sqrt{\lambda}$ (acting as an inverse system size in physical units) to construct an IR and UV scale invariant object \mathcal{O} ,

$$\mathcal{O} = \lambda^{-d_{uv}/2} \Delta^{-d_{ir}} O. \quad (4)$$

Similarly we construct from $\alpha - \alpha_c$ a scale invariant quantity: $\Delta^{-1/\nu}(\alpha - \alpha_c)$.

TABLE I. Summary of all the UV and IR scaling exponents.

	UV exponent	IR exponent
λ	2	0
$\alpha - \alpha_c$	0	$1/\nu = 1$
L^{-1}, δ	1	1
ξ	-1	-1
ϕ	0	$\beta = 1/8$
$\phi^3 - \frac{3}{4\pi}\log(\lambda)\phi$	0	$\beta = 1/8$
$\exp(S)$	$-\frac{c_{uv}}{6} = -\frac{1}{6}$	$-\frac{c_{ir}}{6} = -\frac{1}{12}$

A general data point consists of variables: μ^2, λ , and the bond dimension χ , that map to an observable O . We then do a change of variable of χ to δ or $\Delta = \delta/\sqrt{\lambda}$ with improved scaling properties [12]. Next, those four numbers are transformed to $\Delta^{-1/\nu}(\alpha - \alpha_c), \lambda$, and $\alpha - \alpha_c$, that map to \mathcal{O} , representing a function that, by construction, does not have an explicit dependence on λ , or $\alpha - \alpha_c$. If everything works out, the 4D data can hence be collapsed to a 2D curve,

$$[\mu^2, \lambda, \chi, O] \rightarrow [\Delta^{-1/\nu}(\alpha - \alpha_c), \lambda^{-d_{uv}/2} \Delta^{-d_{ir}} O]. \quad (5)$$

V. CORRECTIONS

The critical point depends strongly on λ when simply using the definition in Eq. (3), which is problematic for the UV- and IR-scaling that we hope to impose. This can be solved by adding corrections to α that make the lattice critical point α_c approximately constant as a function of λ , so that for the newly defined α the critical (red) line and α_c line in Fig. 1 become identical.

We provide α with λ -corrections parametrized as follows:

$$\alpha \rightarrow \alpha + A\lambda \log(\lambda) + B\lambda + C\lambda^2 \log(\lambda)^2 + D\lambda^2 \log(\lambda) + E\lambda^2 + \dots \quad (6)$$

The first two terms have been observed before, see e.g., [11,27], and in the Supplemental Material [26] we show that the mass renormalization from the two-loop setting sun diagram with the lattice regularization (2) indeed produces terms of the form $\lambda \log \lambda/\lambda_0$. The subsequent terms in the series are simply products of the first two.

We also expect corrections for the observables O , since the above described scaling properties only hold true in the limit $\lambda \rightarrow 0$ and $\alpha - \alpha_c \rightarrow 0$. We give the same type of corrections as we considered for α ,

$$O \rightarrow O(A_O + B_O\lambda \log(\lambda) + C_O\lambda + D_O\lambda^2 \log(\lambda)^2 + E_O\lambda^2 \log(\lambda) + F_O\lambda^2 + \dots). \quad (7)$$

These prefactors A_O, B_O, \dots can be given an $\alpha - \alpha_c$ dependence, to provide corrections to the IR behavior. In practice, it will only be needed to give A_O a linear dependence on $\alpha - \alpha_c$, and then only for the entanglement entropy. This type of correction to the IR scaling can be understood as compensating for the following generic form of the power law,

$$O \sim (\alpha - \alpha_c)^{\beta/\nu} (1 + A(\alpha - \alpha_c)^\omega + \dots). \quad (8)$$

The point is now that we have to adjust the parameters A, B, \dots of Eqs. (6) and (7) to make the scaling properties

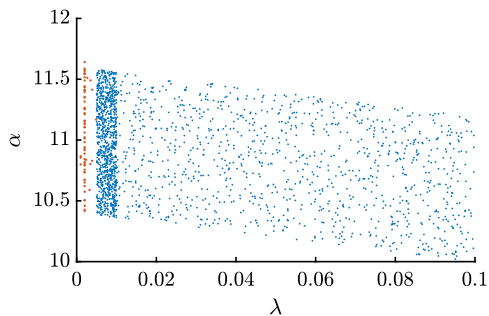


FIG. 2. A plot of the λ and α values used in the fits. The red bar indicates the part of the data that is not included in the preliminary fits and is used to estimate the out-of-sample error.

in Table I hold true in the entire data set; in other words, they will be optimized such as to effectuate an optimal collapse of the data.

VI. FITTING PROCEDURE

We plot the four rescaled observables ξ , ϕ , $\tilde{\phi}^3$ and S versus the rescaled parameter $\Delta^{-1/\nu}(\alpha - \alpha_c)$ [see Eq. (5)], and optimize the average orthogonal distance from those data points to a fit function. The practical details of this are straightforward and presented in the Supplemental Material [26].

Our goal is to optimize the corrections [Eqs. (6) and (7)] discussed in the previous section, and use the $\lambda > 0.001$ data to extrapolate to $\lambda = 0$. There is, however, a clear danger of including too many corrections that will over-optimize the fit for $\lambda \in [0.001, 0.1]$, leading to a bad extrapolation $\lambda \rightarrow 0$. Conversely, the same thing can happen if not enough corrections are included.

To remedy this, we perform all our fits, with various combinations of corrections included, using all but the smallest λ data, indicated in Fig. 2, allowing us to see which fits permit extrapolation to smaller λ . Specifically, our criterion for a ‘good’ set of corrections is that they give a smaller average out-of-sample error than in-sample, for all observables simultaneously.

VII. RESULTS

We calculated 2081 data points, each with a random $\lambda \in [0.001, 0.1]$, associated random α chosen close to the expected critical point, and a random MPS bond dimension $\chi \in [100, 200]$.

We considered 372 different combinations of corrections (6) and (7), deemed reasonable from preliminary fits but varied enough to be unbiased to any specific set of corrections. From this we found 268 fits with a smaller out-of-sample than in-sample error. For all these ‘good’ fits we optimize again, this time using all the data, and plot the values for α_c versus the number of fitting parameters in Fig. 3.

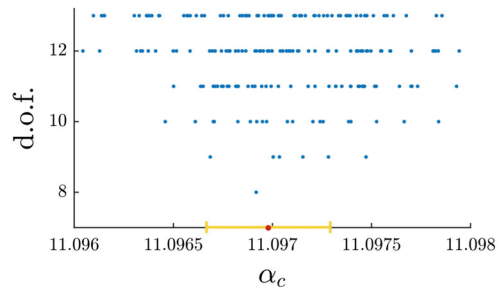


FIG. 3. For the 268 ‘good’ fits (see text); the value of α_c plotted versus the number of fit parameters that were included ($\alpha_c +$ the parameters in the scaling corrections). We use the median to estimate the best value of $\alpha_c = 11.09698(31)$ (indicated with a red dot), and an error bar is estimated with the median distance from that best value (yellow interval).

For a single fit, there is no clear way to estimate the error on α_c with this technique. However, we can use the fact that there are many different fits to get an idea of the error bar, but notice that these different results are not strictly statistical independent. For our final value of α_c we take the median value of all good fits, while for the quoted error bar we take the median distance from this median value of α_c . This final result is compared with previous results in Table II and the collapse plots for the best fit is shown in Fig. 4, and the specific parameters used may be found in the Supplemental Material [26].

From this set of ‘good’ fits, we can conclude that we absolutely need to include $\lambda \log \lambda$ and $\lambda^2 \log \lambda$ terms (those terms were not included in the previous work [12] and are responsible for the suboptimal results there), but it also became clear that the $\lambda^2 \log(\lambda)^2$, $\lambda^3 \log(\lambda)^3$ and $\lambda^3 \log(\lambda)^2$ terms should not be included. $\lambda^3 \log(\lambda)$ and λ^3 could help, but could not improve the out-of-sample error with respect to the set of corrections shown above.

It is interesting to check whether the fit would allow for the calculation of the prefactors of the universal divergent terms (as usually determined by Feynman diagrams). If we fit the renormalization of the ϕ^3 , we find a correction $-0.23888(65) \log(\lambda) \phi$, which should be compared with the analytical $\frac{3}{4\pi} \approx 0.23873$ used previously.

TABLE II. Comparison with some results from the literature.

Method	Year	α_c
MPS [20]	2013	11.064(20)
Hamiltonian truncation [32]	2017	11.04(12)
Borel resummation [33]	2018	11.23(14)
Monte Carlo [10]	2018	11.055(20)
TRG [28]	2019	10.913(56)
gilt-TNR [27]	2020	11.0861(90)
This work	2021	11.09698(31)

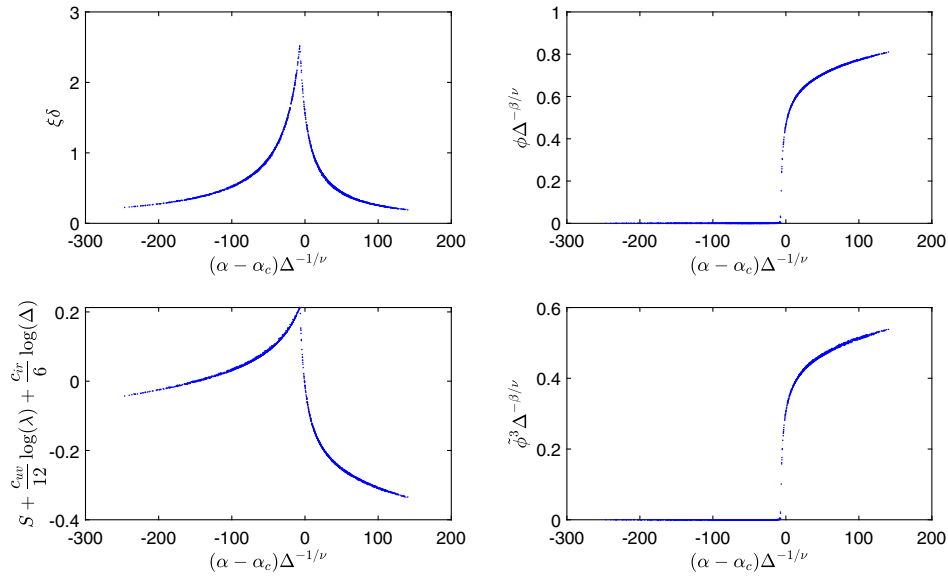


FIG. 4. TOP-LEFT: The rescaled correlation length ξ vs the rescaled coupling $\alpha - \alpha_c$. TOP-RIGHT: The order parameter ϕ vs the rescaled coupling $\alpha - \alpha_c$. BOTTOM-LEFT: The renormalized and rescaled order parameter $\tilde{\phi}^3$ vs the rescaled coupling $\alpha - \alpha_c$. BOTTOM-RIGHT: The logarithmically rescaled entanglement entropy S vs the rescaled coupling $\alpha - \alpha_c$. Note that the shifted singular points of these functions imply a shift in location of the effective critical point by an amount proportional to $\Delta^{-1/\nu}$, this is a general feature found in scaling functions [12].

VIII. CONCLUSION

A critical QFT is something special. Like with any QFT the regulated model becomes UV critical as the cutoff is taken to infinity, but there is also an IR criticality due to the continuum phase transition. It thus has a sort of double criticality, each with a different CFT description. In this work we have shown how, in the case of $\lambda\phi_2^4$, this feature allows for a double scaling analysis, giving rise to collapse plots for the different QFT observables, encapsulating both scaling behaviors in one go. We stress that our approach is general, in the sense that it can be applied to any method that is confronted with both types of scaling, and is not

limited to tensor network based methods. Furthermore, the double scaling approach is not restricted to $D = 2$ space-time dimensions or zero temperature. In particular it would be interesting to explore the double scaling also for $D > 2$ QFTs that exhibit a purported continuous phase transition, e.g., for Monte-Carlo simulations of the finite temperature chiral symmetry breaking transition for $N_f = 2$ massless QCD.

ACKNOWLEDGMENTS

We would like to thank Rui-Zhen Huang for an interesting discussion on scale invariant quantities. This research is supported by ERC Grant No. QUTE (647905) (B. V., F. V.)

-
- [1] Michael E. Fisher and Michael N. Barber, Scaling Theory for Finite-Size Effects in the Critical Region, *Phys. Rev. Lett.* **28**, 1516 (1972).
 - [2] E. Brézin, An investigation of finite size scaling, *J. Phys. (Les Ulis, Fr.)* **43**, 15 (1982).
 - [3] J.L. Cardy, *Finite-Size Scaling*, Current Physics (North-Holland, Amsterdam, 1988).
 - [4] Martin Luscher, Peter Weisz, and Ulli Wolff, A numerical method to compute the running coupling in asymptotically free theories, *Nucl. Phys.* **B359**, 221 (1991).
 - [5] Karl Jansen, Chuan Liu, Martin Luscher, Hubert Simma, Stefan Sint, Rainer Sommer, Peter Weisz, and Ulli Wolff, Nonperturbative renormalization of lattice QCD at all scales, *Phys. Lett. B* **372**, 275 (1996).
 - [6] K. G. Wilson and John B. Kogut, The renormalization group and the epsilon expansion, *Phys. Rep.* **12**, 75 (1974).
 - [7] John B. Kogut, An introduction to lattice gauge theory and spin systems, *Rev. Mod. Phys.* **51**, 659 (1979).
 - [8] Will Loinaz and R.S. Willey, Monte Carlo simulation calculation of critical coupling constant for continuum ϕ^4 in two-dimensions, *Phys. Rev. D* **58**, 076003 (1998).
 - [9] Tomasz Korzec, Ingmar Vierhaus, and Ulli Wolff, Performance of a worm algorithm in theory at finite quartic coupling, *Comput. Phys. Commun.* **182**, 1477 (2011).

- [10] Simone Bronzin, Barbara De Palma, and Marco Guagnelli, New Monte Carlo determination of the critical coupling in ϕ_2^4 theory, *Phys. Rev. D* **99**, 034508 (2019).
- [11] David Schaich and Will Loinaz, An improved lattice measurement of the critical coupling in ϕ_2^4 theory, *Phys. Rev. D* **79**, 056008 (2009).
- [12] B. Vanhecke, J. Haegeman, K. Van Acoleyen, L. Vanderstraeten, and F. Verstraete, Scaling Hypothesis for Matrix Product States, *Phys. Rev. Lett.* **123**, 250604 (2019).
- [13] Ignacio Cirac, David Perez-Garcia, Norbert Schuch, and Frank Verstraete, Matrix product states and projected entangled pair states: Concepts, symmetries, and theorems, *Rev. Mod. Phys.* **93**, 045003 (2021).
- [14] Jutho Haegeman and Frank Verstraete, Diagonalizing transfer matrices and matrix product operators: A medley of exact and computational methods, *Annu. Rev. Condens. Matter Phys.* **8**, 355 (2017).
- [15] M. T. Fishman, L. Vanderstraeten, V. Zauner-Stauber, J. Haegeman, and F. Verstraete, Faster methods for contracting infinite two-dimensional tensor networks, *Phys. Rev. B* **98**, 235148 (2018).
- [16] T. Nishino, K. Okunishi, and M. Kikuchi, Numerical renormalization group at criticality, *Phys. Lett. A* **213**, 69 (1996).
- [17] F. Pollmann, S. Mukerjee, A. M. Turner, and J. E. Moore, Theory of Finite-Entanglement Scaling at One-Dimensional Quantum Critical Points, *Phys. Rev. Lett.* **102**, 255701 (2009).
- [18] L. Tagliacozzo, T. R. de Oliveira, S. Iblisdir, and J. I. Latorre, Scaling of entanglement support for matrix product states, *Phys. Rev. B* **78**, 024410 (2008).
- [19] B. Pirvu, G. Vidal, F. Verstraete, and L. Tagliacozzo, Matrix product states for critical spin chains: Finite-size versus finite-entanglement scaling, *Phys. Rev. B* **86**, 075117 (2012).
- [20] Ashley Milsted, Jutho Haegeman, and Tobias J. Osborne, Matrix product states and variational methods applied to critical quantum field theory, *Phys. Rev. D* **88**, 085030 (2013).
- [21] T. Nishino and K. Okunishi, Corner transfer matrix renormalization group method, *J. Phys. Soc. Jpn.* **65**, 891 (1996).
- [22] R. Orús and G. Vidal, Simulation of two-dimensional quantum systems on an infinite lattice revisited: Corner transfer matrix for tensor contraction, *Phys. Rev. B* **80**, 094403 (2009).
- [23] P. Corboz, S. R. White, G. Vidal, and M. Troyer, Stripes in the two-dimensional t-J model with infinite projected entangled-pair states, *Phys. Rev. B* **84**, 041108 (2011).
- [24] Shau-Jin Chang, Existence of a second-order phase transition in a two-dimensional ϕ^4 field theory, *Phys. Rev. D* **13**, 2778–2788 (1976).
- [25] D. C. Brydges, J. Frohlich, and A. D. Sokal, A new proof of the existence and nontriviality of the continuum ϕ_2^4 and ϕ_3^4 quantum field theories, *Commun. Math. Phys.* **91**, 141 (1983).
- [26] See Supplemental Material at <http://link.aps.org/supplemental/10.1103/PhysRevD.106.L071501> for more details.
- [27] Clement Delcamp and Antoine Tilloy, Computing the renormalization group flow of two-dimensional ϕ^4 theory with tensor networks, *Phys. Rev. Res.* **2**, 033278 (2020).
- [28] Daisuke Kadoh, Yoshinobu Kuramashi, Yoshifumi Nakamura, Ryo Sakai, Shinji Takeda, and Yusuke Yoshimura, Tensor network analysis of critical coupling in two dimensional ϕ^4 theory, *J. High Energy Phys.* **05** (2019) 184.
- [29] Here we use the term ‘observables’ for quantities exhibiting a well posed continuum limit. The entanglement entropy is not an observable in the quantum information theoretic sense [30].
- [30] Michael A. Nielsen and Isaac L. Chuang, *Quantum Computation and Quantum Information: 10th Anniversary Edition*, 10th ed. (Cambridge University Press, USA, 2011).
- [31] Pasquale Calabrese and John Cardy, Entanglement entropy and quantum field theory, *J. Stat. Mech.* (2004) P06002.
- [32] Joan Elias-Miro, Slava Rychkov, and Lorenzo G. Vitale, High-precision calculations in strongly coupled quantum field theory with next-to-leading-order renormalized Hamiltonian truncation, *J. High Energy Phys.* **10** (2017) 213.
- [33] Marco Serone, Gabriele Spada, and Giovanni Villadoro, $\lambda\phi^4$ theory—Part I. The symmetric phase beyond NNNNNNNLO, *J. High Energy Phys.* **08** (2018) 148.